Moroccan Journal of Chemistry
ISSN: 2351-812X
http://revues.imist.ma/?journal=morjchem&page=login
F. Shojaie / Mor. J. Chem. 6 N°4 (2018) 676-688

Arsine adsorption on the surface of palladium-doped carbon nanotubes

F. Shojaie

Department of Photonic, Institute of Science and High Technology and Environmental Sciences, Graduate University of Advanced Technology, PO Box 76315-117, Kerman, Iran

** Corresponding author:*
f.shojaie@kgut.ac.ir
Received 23 Nov 2017,
Revised 18 Dec 2018,
Accepted 20 Dec 2018

Abstract

Density functional theory was used to investigate arsine interactions with palladium-doped single-walled carbon nanotubes (Pd/SWCNTs). Adsorption energies, quantum descriptors, bond order, atomic charge, optical properties, and electrostatic potential of Pd/SWCNTs, arsine and arsine-Pd/SWCNT complexes were calculated. The results show arsine is weakly bonded to Pd/SWCNTs through van der Waals type interactions. The interaction between Pd and Pd/SWCNT is physisorption as the binding energy and charge transfer are small, and adsorption distance is large. The electronic transitions from the highest occupied molecular orbital (HOMO) to the lowest unoccupied molecular orbital (LUMO) (H→L) have the maximal wavelength and the lowest oscillator strength

Keywords: *Arsine, Pd/SWCNTs, Adsorption energies, bond order analysis.*

1.Introduction

Arsine is a gas with the formula AsH_3. Arsine is the most dangerous arsenic compound and highly toxic [l]. In industry, this gas has been produced during smelting and refining of metals. Arsine poisoning has been reported in galvanizing, soldering, etching and lead plating operations[2]. Arsine can be produced by fungi, especially in sewage, in the presence of arsenic[2, 3]. Coal contains considerable quantities of arsenic and thus arsine can be formed in the conversion process of coal to gas and other reactions by-products[3]. There are many reports on workers who have been poisoned by arsine. Serious health problem can be triggered by arsine even if a small amount of this substance is ingested by human body [4-7]. Arsine is commercially produced and is used in organic synthesis, semiconductor industry and catalytic processes. Arsine is highly poisonous, colorless and soluble in water. Removal of arsine from a gas phase is an important matter especially in industry[8].Thus, finding an effective method to remove arsine is essential. There are specific adsorbers which can be used to remove arsine gas from different environments. A great deal of efforts have been dedicated to find methods to remove arsine from various media. Examples of such methods are use of alumina [9], activated carbons supports[10] and doping CuO with carbon[11]. Petit et al investigated the role of oxygen and sulfur-containing groups on non-impregnated activated carbons in the retention/oxidation of arsine[12]. Kunaseth et al used DFT to study adsorption of arsine and its dehydrogenated products (AsH_2, AsH, As) on the palladium doped single-vacancy defective graphene surface[13]. The interesting properties of nanotubes have caused researchers and companies to consider their uses in several fields and in particular their excellent use as gas adsorbers. Some studies have indicated that chemical doping of carbon nanotubes can enhance their gas absorbing properties. In this work the DFT will be used to investigate the arsine interactions with Pd/SWCNTs. Pd/SWCNTs have not yet been used as sensors for arsine detection. The aim of our study is to use the DFT to investigate the role of doped Pd atom in arsine adsorption. We have studied adsorption energies, quantum descriptors, bond order analysis, atomic charge analysis, optical properties, and electrostatic potential of Pd/SWCNTs and arsine. A comparison between the characteristics of the Pd/SWCNTs and arsine can provide novel information about mechanism of arsine adsorption on the surface of Pd/SWCNTs.

2. Computational performance

All calculations were performed using DMol3 code in Materials Studio 5.5. The Perdew-Wang (PW91) method of the generalized gradient approximation (GGA) and the double numerical plus polarization (DNP) function were used in all calculations for geometrical optimization. Total energy convergence criteria for self-consistent field (SCF) were set to 10−6 eV. The structures and the optimized configurations of compounds were considered to be minima based on the absence of imaginary frequencies. A smearing of 0.005 Hartree and 10 Pulay direct inversion of the iterative subspace (DIIS)[14] were considered to improve computational performance in terms of fast SCF convergence. The basis set superposition errors (BSSE) of the DNP have been used for the counterpoise correction of the interaction energy[15]. The Pd-doped C (5, 5) pristine carbon nanotubes containing 80 carbon atoms and 20 hydrogen atoms (C80H20) were used in this work. The C (5, 5) carbon nanotube is the most reactive nanotube[16]. The bond length between two carbon atoms in SWCNTs is 1.42 Å which is equal to a bond length between two carbon atoms in sp2 hybridization. The diameter and the length of the nanotubes are 6.78 and 9.84 Å respectively. To study the effect of doped Pd atom on the adsorption of arsine gas, we have considered ten stable structures of arsine-Pd/SWCNT complexes. The optimized configurations of these models are shown in Figure 1.

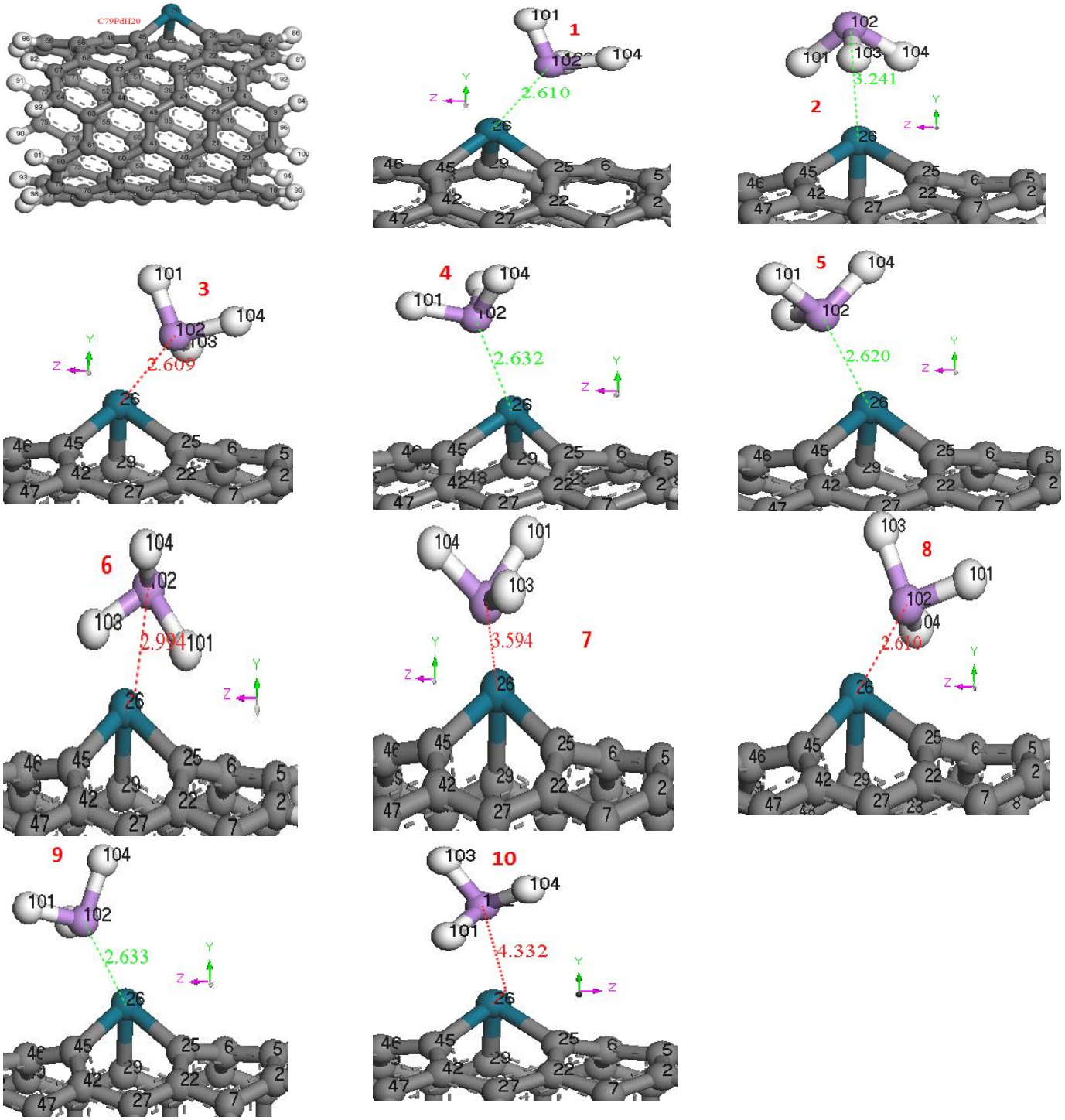

Figure 1. Frontal views of the equilibrium configurations of AsH3 adsorption on the surface of Pd-doped (5, 5) armchair model of SWCNT. The violet, the blue-green, the white and the gray atoms represent arsenic, palladium, hydrogen and carbon respectively.

3. Results and Discussions

3.1. Geometrical Parameters

Quantum chemical parameters give information on chemical reactivity of molecules. The gap (ΔE) between their highest occupied molecular orbital (HOMO) and lowest unoccupied molecular orbotal (LUMO) energy levels is an important function of reactivity of a molecule. The computed energy gaps of the pristine carbon nanotube and

Pd/SWCNT are 0.931eV [17] and 0.301eV respectively. C79PdH20 electrons need less energy to make a transition from the valance band to the conduction band in comparison to C80H20 and C79NH20 electrons [17]. It seems that the presence of a doping material can increase electrical conductivity. Pd/SWCNT is a more appropriate compound than its pristine carbon nanotube for interactions with arsine. Table 1 shows arsine has higher ELUMO, energy gap and global hardness (η= (I-A)/2, I=-EHOMO) than C79PdH20 but lower electron affinity (A=-ELUMO), electronegativity (χ = (I+A)/2) and global softness (σ=1/η). The electrophilicity (ω = χ2/2η) of C79PdH20 is about 32 times greater than the arsine. The C79PdH20 can act as an electrophile when interacting with nucleaphilic arsine. Arsine is suitable for electrophilic attack. The C79PdH20 has sites for adsorption of nucleophilic agent. The highest Fukui index of C79PdH20 (f+) is associated with Pd atom. The arsine site for electrophilic attack is the arsenic atom. The key Fukui indices of the C79PdH20 (f+) and arsine (f-) are listed in Table 2. Therefore, conformations of the arsine-Pd/SWCNT complexes were considered. These conformations were optimized by the GGA/PW91 method in gas phase. We have studied ten stable configuration of arsine-Pd/SWCNT complexes. Figure 1 shows Pd/SWCNT structure and the ten optimized configurations of arsine-Pd/SWCNT complexes which are referred to models number 1 to 10.

Table 1. Quantum Chemical Descriptors for AsH3 and Pd/SWCNT.

Models	**η (eV)**	**E_{LUMO} (eV)**	**ΔE (eV)**	**X (eV)**	**ω (eV)**
AsH_3	3.533	-0.123	7.067	3.656	1.891
Pd/SWCNT	0.151	-4.113	0.301	4.264	60.348

Table 2. Calculated Fukui Functions for arsine and Pd/SWCNT

Models	**Atoms**	**f^+**		**f^-**	
		Mulliken	Hirshfeld	Mulliken	Hirshfeld
AsH_3	As	0.460	0.564	0.348	0.503
	H	0.180	0.145	0.217	0.166
	Pd	0.045	0.063	0.055	0.065
	C25	0.015	0.013	0.014	0.013
Pd/SWCNT	C45	0.033	0.023	0.034	0.023
	C29	0.007	0.008	0.007	0.008

Figure 2 shows the energy gaps of optimized Pd/SWCNT and arsine-Pd/SWCNT complexes. The model numbers 2, 4 and 7 have less energy gaps than other models. The energy gap of model number 2 is lower than those of model numbers 4 and 7. The model number 2 is characterized as a soft molecule based on its absolute hardness and softness parameters and has a higher reactivity than other models (See Table 3). The models numbers 2, 4 and 7 have more electronegativity than other models and C79PdH20. The model number 2 is more electrophilic than model numbers 4 and 7. The Fermi energies of all the models are located between their highest occupied molecular orbital (HOMO) and lowest unoccupied molecular orbotal (LUMO) energies.

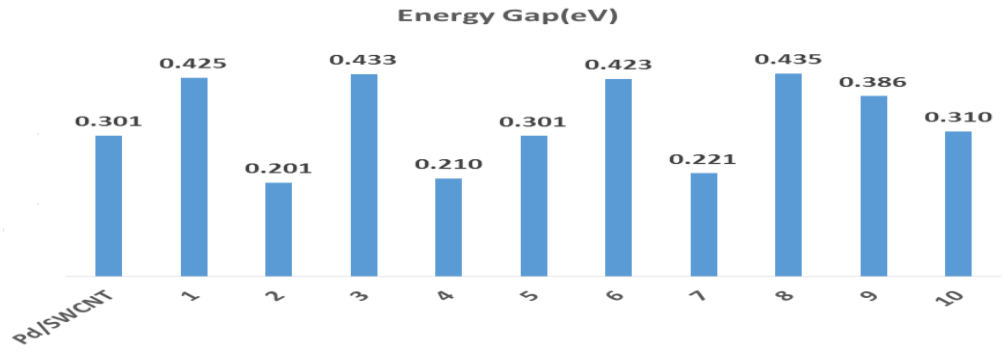

Figure 2. Diagram of energy gap for Pd/SWNT and AsH_3- Pd/SWNT models.

Table 3. The global softness and electrophilicity for the studied compound

Models	σ (eV^{-1})	ω(eV)
Pd/SWCNT	6.638	60.348
1	4.706	40.931
2	9.945	89.784
3	4.620	40.155
4	9.533	84.579
5	6.645	58.219
6	4.728	40.950
7	9.050	81.550
8	4.598	39.916
9	5.179	45.093
10	6.449	58.354

Figure 3 shows the density of states (DOS) of spin up and spin down electrons in Pd/SWCNT and the 10 models. The DOSs of spin up and spin down electrons are equal for all electron energies. This means that all structures of arsine-Pd/SWCNT models are antiferromagnetic. Thus, the adsorption of arsine has no effect on the magnetic properties of Pd/SWCNT.

The transitions between electronic states may be approximately interpreted in terms of one-electron transitions. The quantum calculations on electronic absorption spectra were performed. Figure 4 shows oscillator strength values which were calculated by TD-DFT. Table 4 shows oscillator strength and wavelength of electronic transitions of band gap (H→L) and also electronic transitions that have maximal oscillator strength. The electronic transitions from the HOMO to the LOMO (H→L) have the maximal wavelength and the lowest oscillator strength (See Table 4). The wavelength of transitions from H to L for the C (5, 5) carbon nanotubes is lower than Pd-doped nanotube that is the presence of a doping material can increase absorption wavelength. The electronic transitions results are in good agreement with energy gap data. Figure 4 shows that minimum wavelength of SWCNT is in the 544 nm region, which corresponds to a 2.28 eV. This absorption corresponds to a transition from the four orbital below the HOMO (H-4) to the LOMO (L). For Pd-doped nanotube, the transition from H-2 to L-2 has a minimum wavelength that is located in the 705 nm region (1.76eV). The maximal wavelength of transition of H→L in model number 2 is higher than other models and Pd/SWCNT. This model has a minimum wavelength in the 731 nm region, which corresponds to a transition of H-4→L.

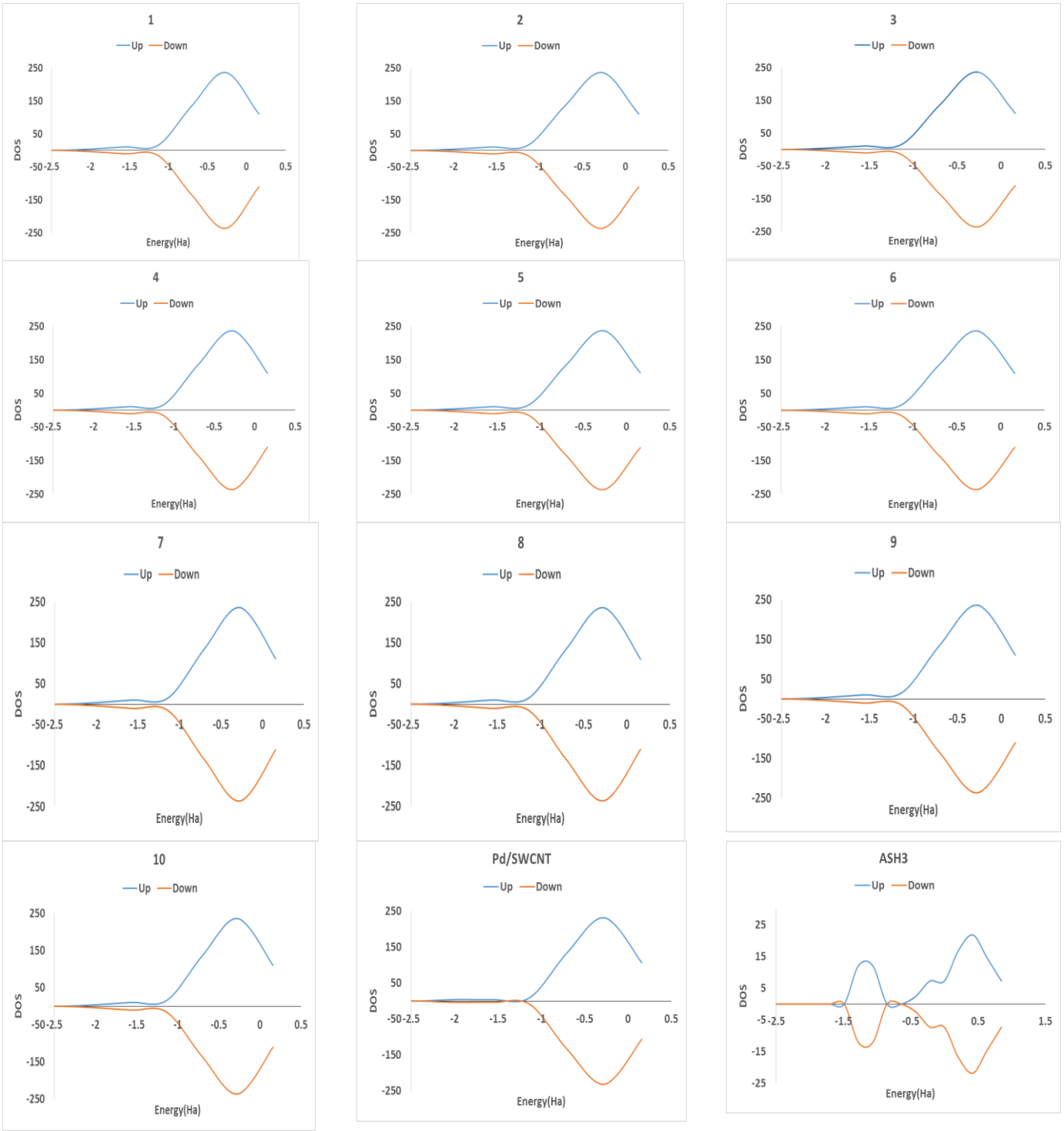

Figure 3. The DOS of spin up and spin down electrons of Pd/SWNT, AsH_3 and AsH_3- Pd/SWNT models.

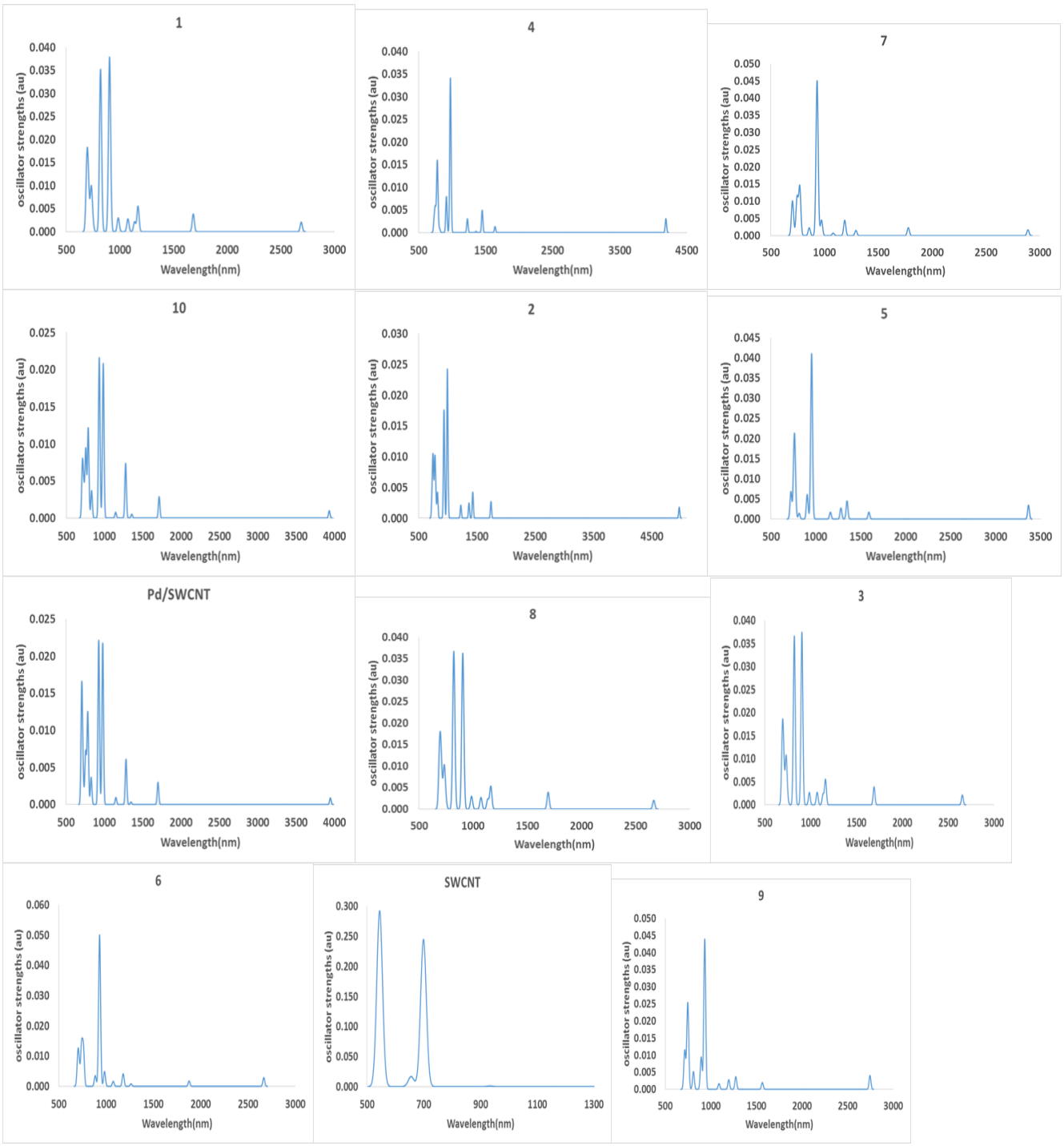

Figure 4. The oscillator strength values in terms of wavelength which were calculated by time-dependent density-functional theory (TD-DFT).

The transitions from the first orbital below the HOMO (H-1) to the first orbital above the LOMO (L+1) have the most intense peaks in model numbers 1, 3, 6, 7 and 10 and Pd/SWCNT (See Table 4). The maximal oscillator strength occurs at transitions from H to L+6 for the SWCNT. The most intense peaks are located between the HOMO and the third orbital above the LOMO in model numbers 2, 4, 5 and 9. In model number 8, transitions of H-2→L+1 have maximal oscillator strength.

Table 4. The oscillator strength and wavelength of electronic transitions of H→L and wavelength of electronic transitions with maximal oscillator strength

Models	Transition	λ(nm)	Oscillator strength	Models	Transition	λ(nm)	Oscillator strength
SWCNT	H→L	1272	0.0000	5	H→L	3366	0.0034
	H→L+6	545	0.1490		H→L+3	953	0.0410
Pd/SWCNT	H→L	3947	0.0009	6	H→L	2665	0.0029
	H-1→L+1	926	0.0221		H-1→L+1	931	0.0500
1	H→L	2690	0.0021	7	H→L	2890	0.0017
	H-1→L+1	904	0.0379		H-1→L+1	930	0.0450
2	H→L	4968	0.0018	8	H→L	2667	0.0020
	H→L+3	994	0.0243		H-2→L+1	821	0.0367
3	H→L	2653	0.0021	9	H→L	2743	0.0040
	H-1→L+1	905	0.0375		H→L+3	933	0.0439
4	H→L	4187	0.0031	10	H→L	3930	0.0010
	H→L+3	975	0.0341		H-1→L+1	930	0.0216

Table 5. Mayer Bond Order (MBO) and Bond Length (BL) (Å) of studied compounds.

	X-C25		X-C29		X-C45		As-H101		As-H103		As-H104	
	MBO	**LB**	**MBO**	**LB**	**MBO**	**LB**	**MBO**	**LB**	**MBO**	**LB**	**MBO**	**LB**
AsH3	-	-	-	-	-	-	0.985	1.524	0.985	1.524	0.985	1.524
SWCNT(X=C26)	1.202	1.427	1.282	1.415	1.176	1.433	-	-	-	-	-	-
Pd/SWCNT(X=Pd)	0.903	1.974	0.712	2.072	0.882	1.978	-	-	-	-	-	-
1	0.821	2.027	0.688	2.091	0.858	1.978	1.000	1.514	1.000	1.518	1.000	1.509
2	0.849	1.986	0.656	2.104	0.829	1.994	1.000	1.527	1.000	1.567	1.000	1.527
3	0.820	2.027	0.688	2.091	0.858	1.978	1.000	1.514	1.000	1.510	1.000	1.356
4	0.863	1.972	0.641	2.125	0.800	2.022	1.000	1.510	1.000	1.515	1.000	1.516
5	0.867	1.978	0.668	2.099	0.805	2.019	1.000	1.512	1.000	1.512	1.000	1.513
6	0.831	1.997	0.685	2.085	0.845	1.991	1.000	1.555	1.000	1.540	1.000	1.524
7	0.838	1.992	0.663	2.094	0.836	1.993	1.000	1.526	1.000	1.570	1.000	1.527
8	0.819	2.027	0.689	2.091	0.858	1.978	1.000	1.510	1.000	1.514	1.000	1.510
9	0.863	1.979	0.689	2.091	0.801	2.024	1.000	1.512	1.000	1.511	1.000	1.512
10	0.879	1.978	0.713	2.078	0.894	1.978	1.000	1.522	1.000	1.525	1.000	1.524

In order to characterize the X-C (X=C26 in SWCNT and X=Pd in Pd/SWCNT) and As-H bonds in Pd-doped nanotube, pristine SWCNT and AsH3-Pd/SWCNT, the bond lengths (LB) and Mayer bond order (MBO) were calculated (See Table 5). The bond length of Pd-C is longer than its pristine form in Pd-doped nanotubes which indicates the C–C bonds are highly covalent. There are very small differences between the Pd-C25, Pd-C29 and Pd-C45 bond lengths. However, the Pd–C29 bond is slightly weaker than Pd-C25 and Pd-C45 bonds because its length is longer and has a smaller bond order value. The MBO ranges of Pd-C25, Pd-C29 and Pd-C45 bonds in Pd/SWCNT and AsH3-Pd/SWCNT models are 0.819−0.930, 0.641-0.712 and 0.801-0.894 respectively which indicates the Pd atom forms a single bond with C atom. The bond length of Pd-C of AsH3-Pd/SWCNT is longer than Pd-doped nanotubes

and SWCNT. The MBO of As-H in AsH3-Pd/SWCNT is 1.000 and is higher than the MBO of AsH3. There are very small differences between the As-H101, As-H103 and As-H104 bond lengths. The AsH3 adsorption on Pd-loaded SWCNTs shows that changes in the Pd–C bond lengths are greater than the changes in As-H bond lengths.

Table 6 shows the adsorption energies (Eads), equilibrium distances (D) and charge transfers (QT) of the AsH3-Pd/SWCNT models. The small binding energy, large adsorption distance and small charge transfer indicate that AsH3 is weakly bounded to Pd-doped carbon nanotube through van der Waals type interactions. Therefore, these interactions can be identified as physisorption. The adsorption energies of model number 2 and 7 lowest and this means the models number 2 and 7 have lowest thermodynamic stability. Negative values of Eads denote exothermic adsorption.

Table 6. The adsorption energies, equilibrium distances and charge transfers for the AsH_3-Pd/SWCNT models.

System	E_{ads}(eV)	D(Å) As-Pd	Q_T(e)	
			Mulliken	**Hirshfeld**
1	-0.779	2.610	0.003	0.001
2	-0.337	3.241	0.011	-0.004
3	-0.773	2.609	0.003	-0.002
4	-0.684	2.632	-0.017	0.011
5	-0.738	2.620	0.006	-0.004
6	-0.397	2.994	-8.05E-16	1.32E-16
7	-0.333	3.236	0.009	-0.006
8	-0.762	2.610	0.006	-0.004
9	-0.735	2.633	0.004	-0.007
10	-0.433	4.332	0.002	-0.001

The charges which were calculated by Mulliken and Hirshfeld methods, are listed in Table 7. The charges on C25, C26, C29 and C45 atoms of SWCNTs, calculated by Mulliken and Hirshfeld methods, are approximately identical. The charges on C25, C29 and C45 atoms become negative after SWCNTs are doped with palladium. The negative charge could be due to carbon atom being more electronegative than the palladium atom. Table 7 shows the negative charges on the C29 atom of the C79H20Pd are higher than the charges on C25 and C45. These charges are in agreement with their bond lengths. The charge of Pd changes from o.327 in the C79PdH20 to 0.088, 0.260, 0.087, 0.124, 0.109, 0.197, 0.308, 0.088, 0.106 and 0.315 in the models by Mulliken, and from 0.533 to 0.438, 0.500, 0.437, 0.417, 0.424, 0.489, 0.537, 0.437, 0.428 and 0.530 by Hirshfeld, whereas that of As charges decrease by two methods. These analyses indicated that charges transferred from AsH3 to Pd-doped carbon nanotube.

Table 7. The calculated charges by Mulliken and Hirshfeld for studied compounds.

System	X		C25		C29		C45		AsH_3		As	
	Mulliken	**Hirshfeld**	**Mulliken**	**hirshfeld**	**Mulliken**	**hirshfeld**	**Mulliken**	**hirshfeld**	**Mulliken**	**hirshfeld**	**Mulliken**	**hirshfeld**
AsH_3	-	-	-		-		-		0.000	0.002	-0.258	0.047
SWCNT (X=C26)	0.004	-0.002	0.004	-0.001	0.004	-0.002	0.003	-0.002	-		-	-
Pd/SWCNT (X=Pd)	0.327	0.533	-0.184	-0.075	-0.256	-0.129	-0.198	-0.080	-		-	-
1	0.088	0.438	-0.154	-0.071	-0.207	-0.112	-0.200	-0.089	0.267	0.135	-0.080	0.088
2	0.260	0.500	-0.156	-0.065	-0.241	-0.127	-0.175	-0.072	0.053	0.007	-0.251	0.091
3	0.087	0.437	-0.155	-0.072	-0.206	-0.111	-0.199	-0.089	0.267	0.135	-0.079	0.088
4	0.124	0.417	-0.160	-0.070	-0.216	-0.121	-0.166	-0.072	0.202	0.118	-0.139	0.077
5	0.109	0.424	-0.175	-0.079	-0.207	-0.115	-0.166	-0.073	0.233	0.136	-0.115	0.087
6	0.197	0.489	-0.181	-0.078	-0.211	-0.110	-0.177	-0.075	0.147	0.060	-0.256	0.112
7	0.308	0.537	-0.183	-0.076	-0.241	-0.118	-0.194	-0.079	0.051	0.005	-0.204	0.082
8	0.088	0.437	-0.156	-0.072	-0.206	-0.111	-0.198	-0.089	0.267	0.135	-0.080	0.088
9	0.106	0.428	-0.175	-0.079	-0.196	-0.104	-0.177	-0.077	0.238	0.135	-0.113	0.085
10	0.315	0.530	-0.197	-0.077	-0.254	-0.128	-0.184	-0.074	0.014	0.000	-0.269	0.035

The molecular electrostatic potential (MEP) maps are essential in studying and predicting the reactive sites for electrophilic and nucleophilic attacks. The MEP maps were evaluated at the GGA/PW91 level for two directions and are shown in Figure 5. The positive regions of MEP map, shown in blue colour, are related to nucleophilic reactivity and the negative regions, shown in yellow colour, are associated with electrophilic reactivity. This figure shows that the electrostatic potential (ESP) charges of Pd in the models numbers 1, 3, 4, 5, 8 and 9 are more negative than other models. The Hirshfeld and Mulliken charges on the Pd atom of the models numbers 2,7,10 are greater than other models. These results are in good agreement with the ESP charges. The contour map of ESP of Pd-As-H as a function of the bond length is shown in Figures 6. This figure reveals that the charge distribution increases with decreasing bond length between As and Pd atoms.

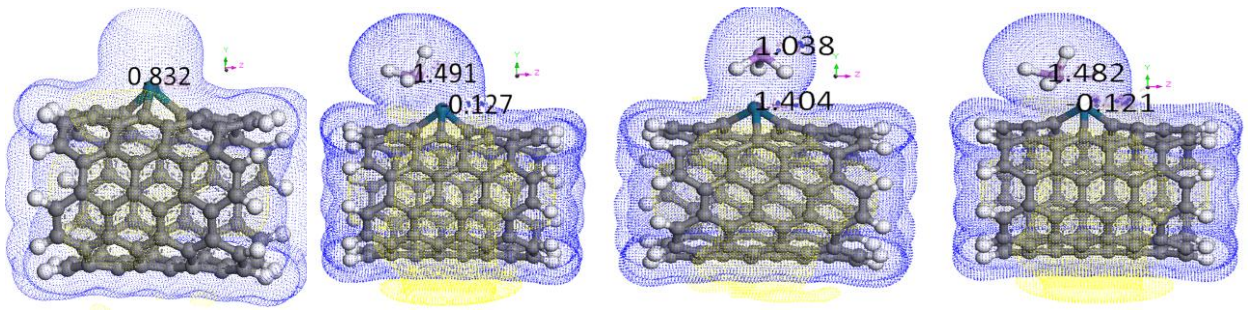

Pd/SWCNT 1 2 3

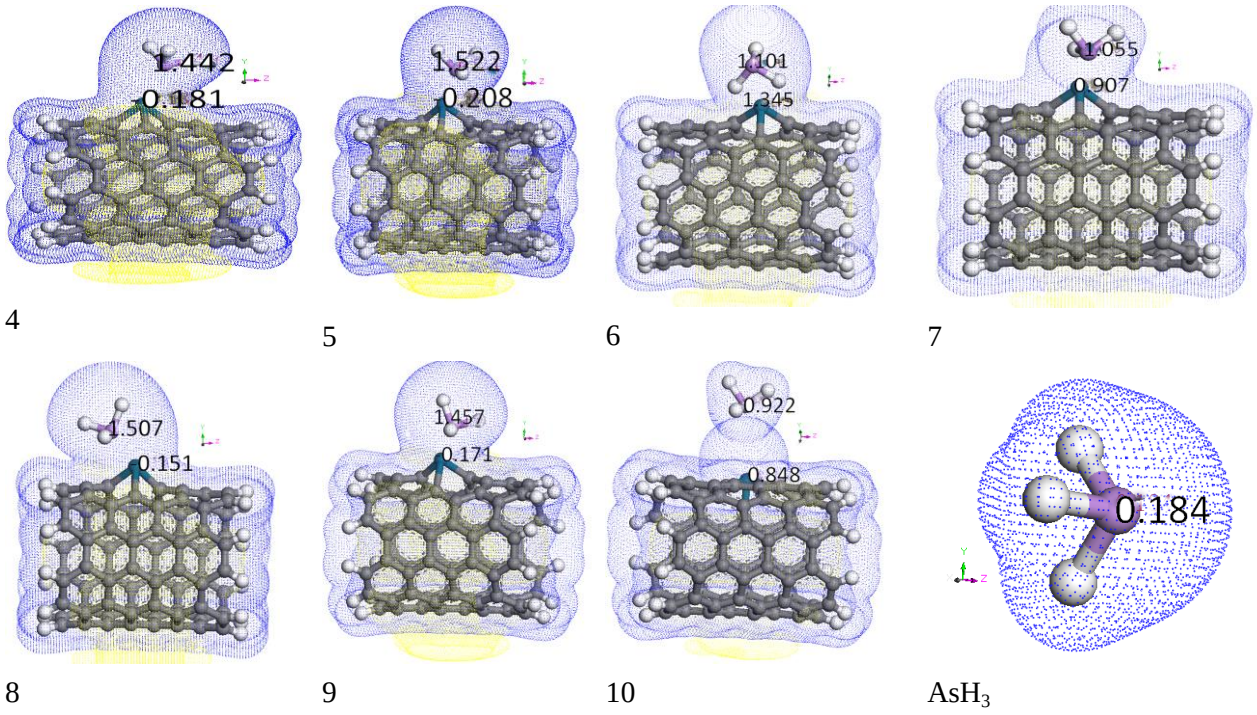

Figure 5. ESP isosurface of compounds studied (isovalue = 0.016, positive values by blue, negative by yellow color DMol^3 / PW91). The numbers are ESP charges for Pd and As.

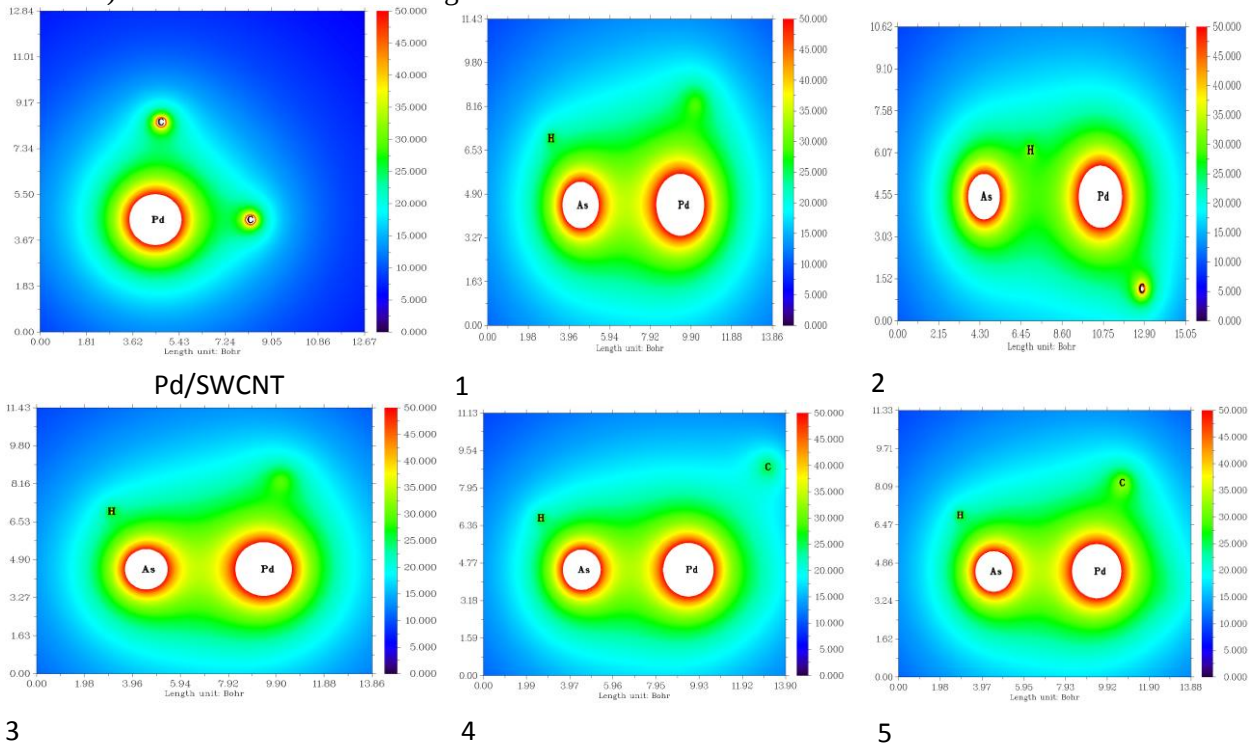

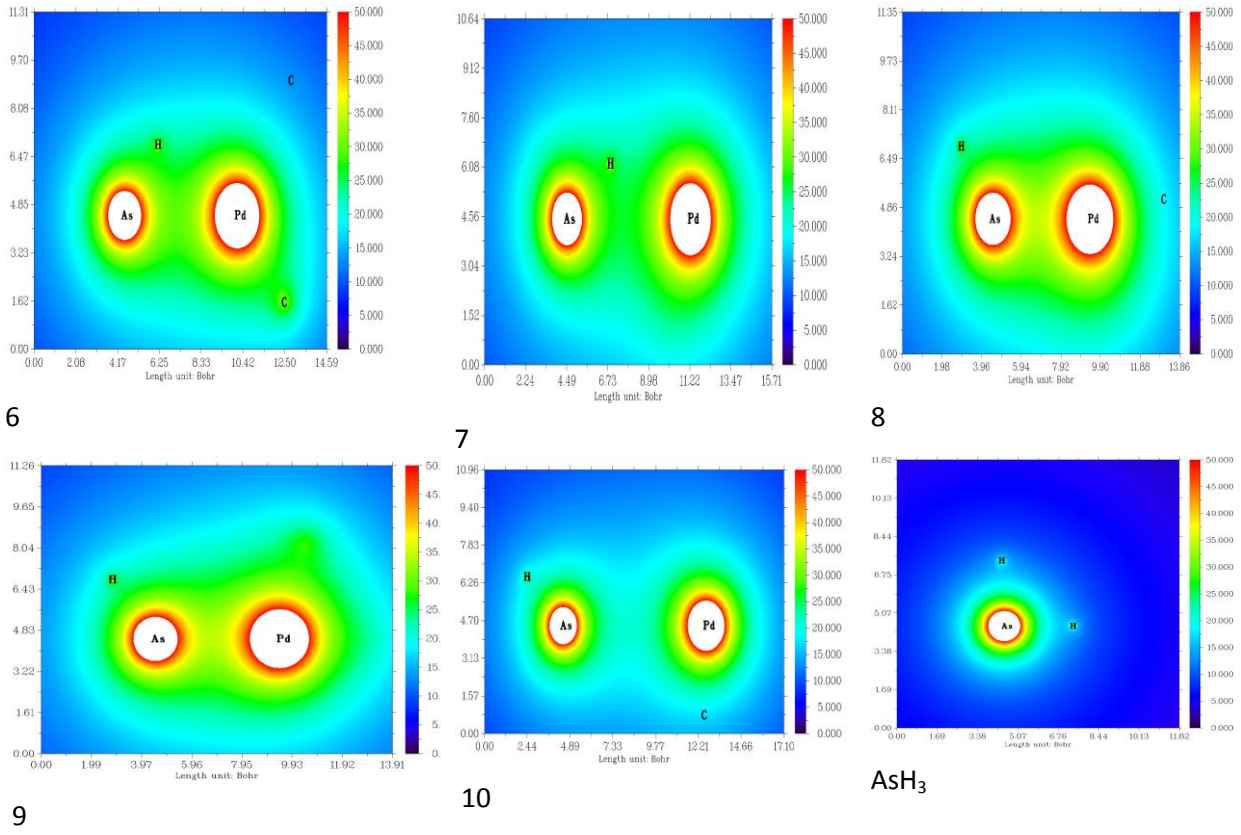

Figure 6. The contour map of electrostatic potential of geometrically optimized Pd-As-H.

4. Conclusion

Computational chemistry simulations were carried out for AsH3-Pd/SWCNT complexes. The Mulliken population analysis revealed that the charge transfer occurred from AsH3 to Pd-doped carbon nanotube. The adsorption process of all AsH3-Pd/SWCNT complexes is exothermic because the adsorption energy values are negative. The AsH3 is weakly bounded to Pd-doped carbon nanotube through van der Waals type interactions. The interaction between Pd and Pd/SWCNT is physisorption because the interaction has a small binding energy, a large adsorption distance and a small charge transfer. The results indicate that the adsorption energies of the AsH3-Pd/SWCNT model number 2 and 7 are the highest among all the models. This means that these two models have lowest thermodynamic stability. Equilibrium distance of model number 2 is more than model number 7. The energy gaps of models numbers 2, 4 and 7 are less than other models and the energy gap of the model 2 is less than models number 4 and 7. The Fermi energy of C79PdH20 and its models are located between HOMO and LUMO energies and the C80H20 Fermi energy is the same as its HOMO energy. The energy gap of C79PdH20 is lower than its pristine form. The presence of a doping material can increase conductivity. The DOSs of spin up and spin down electrons are equal for all values of electron energies. The Pd/SWNT and AsH3-Pd/SWNTs are anti-ferromagnetic. The electronic transitions from the HOMO to the LUMO (H→L) have the maximal wavelength and the lowest oscillator strength in each structure. The maximal wavelength of transition of H→L in model number 2 is higher than other models and Pd/SWCNT. The results show that the presence of a doping material can increase absorption wavelength. In addition, calculations of bond order analysis, atomic charge analysis, and electrostatic potential were carried out.

Acknowledgements- This work was supported by 1527 project from the Department of Photonic, Institute of Science, High Technology & Environmental Sciences, Graduate University of Advanced Technology, Kerman, Iran.

References

[1] M. F. Hughes, B. D. Beck, Y. Chen, A. S. Lewis ,D. J. Thomas, *Toxicological Sciences*., 123 (2011) 305-332.

[2] J. Brighton, Natural Forms of Defense Against Biological, Chemical and Nuclear Threats, Trafford Publishing., 2002.

[3] R. C. Ropp, Encyclopedia of the alkaline earth compounds, Newnes., 2012.

[4] J. Saha, A. Dikshit, M. Bandyopadhyay , K. Saha, Crit. Rev. Env. Sci. Tec., 29 (1999) 281-313.

[5] J. R. Meliker, R. L. Wahl, L. L. Cameron, J. O. Nriagu, Environ. Health., 6 (2007) 1.

[6] Y. Chen, F. Parvez, M. Gamble, T. Islam, A. Ahmed, M. Argos, J. H. Graziano, H. Ahsan, Toxicol Appl Pharmacol., 239 (2009) 184-192.

[7] M. Argos, F. Parvez, Y. Chen, A. I. Hussain, H. Momotaj, G. R. Howe, J. H. Graziano, H. Ahsan, Am. J. Public. Health., 97 (2007) 825-831.

[8] T. S. S. Dikshith, Handbook of chemicals and safety, CRC Press, 2016.

[9] N. Carr, D. STAHFELD, H. Robertson, Hydrocarb. Process., 64 (1985)100-102.

[10] T. Watanabe, H. Imai and T. Suzuki, J. Electrochem. Soc., 143 (1996) 2654-2657.

[11] R. Quinn, T. A. Dahl, B. W. Diamond, B. A. Toseland, Ind. Eng. Chem. Res, 45 (2006) 6272-6278.

[12] C. Petit, G. W. Peterson, J. Mahle, T. J. Bandosz, Carbon, 48 (2010) 1779-1787.

[13] M. Kunaseth, T. Mudchimo, S. Namuangruk, N. Kungwan, V. Promarak, S. Jungsuttiwong, Appl. Surf. Sci., 367 (2016) 552-558.

[14] P. Pulay, J. Comput. Chem., 3 (1982) 556-560.

[15] Y. Inada and H. Orita, J. Comput. Chem., 29 (2008) 225-232.

[16] X. Lu, F. Tian, X. Xu, N. Wang, Q. Zhang, J. Am. Chem. Soc., 125 (2003)10459-10464.

[17] F. Shojaie, Phys. Chem. Res., 4 (2016) 451-467.